Valence band structure of $HgTe/Hg_{1-x}Cd_xTe$ single quantum wells

K. Ortner, X. C. Zhang, A. Pfeuffer-Jeschke, C. R. Becker,* G. Landwehr, and L. W. Molenkamp
Physikalisches Institut der Universität Würzburg, Am Hubland, 97074 Würzburg, Germany
(Received 19 February 2002; published 15 August 2002)

Properties of the valence-band structure of modulation-doped type-III $HgTe/Hg_{1-x}Cd_xTe(001)$ quantum wells (QW's) have been studied by means of magneto-transport experiments and self-consistent Hartree calculations using the full 8×8 $\boldsymbol{k}\cdot\boldsymbol{p}$ Hamiltonian in the envelope-function approximation. A metallic top gate was used in order to investigate the band structure by varying the hole concentration or the Fermi energy. This resulted in direct experimental evidence of an indirect band gap in a quantum well with an inverted band structure. The Kramers degeneracy for finite $\boldsymbol{k}$ is removed, and only one spin-orbit split valence subband is occupied due to the indirect band structure. The fourfold symmetry of the $H2$ valence band at finite values of $\boldsymbol{k}_\parallel$ is also reflected in a QW with a normal band structure, whose $H1$ valence band has four occupied secondary maxima at finite values of $\boldsymbol{k}_\parallel$ in addition to the central maximum.

DOI: 10.1103/PhysRevB.66.075322 PACS number(s): 73.21.Fg, 73.61.Ga, 71.20.Nr

I. INTRODUCTION

$HgTe/Hg_{1-x}Cd_xTe$ heterostructures are type-III structures which are formed by a semiconductor and a zero-gap semiconductor or semimetal. By variation of the width of the HgTe well, d_w, it is possible to fabricate a semiconductor with either a normal or an inverted subband structure. *n*-type modulation-doped $HgTe/Hg_{0.3}Cd_{0.7}Te(001)$ single quantum wells (SQW's) have been successfully grown in recent years,[1] exhibiting large Hall mobilities, pronounced Shubnikov–de Haas (SdH) oscillations and well-developed quantum Hall plateaus. Typical electron effective masses[2] as low as $0.02m_0$, as a result of the small energy gap and a Landé g factor[3] of about -20, have been determined. Interesting phenomena have been observed including a large Rashba spin-orbit splitting in quantum wells (QW's) with an inverted band structure[4] and the persistence of quantum Hall plateaus up to 60 K.[5]

Magnetoabsorption[3,6] and absorption[7] investigations have yielded information about intersubband transitions which involve both the conduction and valence bands. As mentioned above, the band structure of the conduction bands has been the subject of recent investigations; however, to date no detailed experimental, e.g., magnetotransport, results for *p*-type HgTe QW's have been published which could give direct information about the valence-band structure. The lack of magnetotransport results is primarily due to the fact that heavy-hole effective masses are larger than electron effective masses, and as a result samples have lower carrier mobilities. On the other hand, transport investigations of high-quality *p*-type QW's are highly desirable in order to elucidate the complex valence band structure of the type-III $HgTe/Hg_{1-x}Cd_xTe$ system. This valence-band structure has been the subject of investigations of mixed conductivity in $HgTe/Hg_{1-x}Cd_xTe$ multiple quantum wells and superlattices.[8–10] Using the modulation doping technique it is now possible to manufacture two-dimensional hole gases in $HgTe/Hg_{1-x}Cd_xTe(001)$ QW's with sufficiently high mobilities.[13]

In the present investigation, magnetotransport data for this system have been quantitatively described using self-consistent Hartree calculations based on Kane's 8×8 $\boldsymbol{k}\cdot\boldsymbol{p}$ model.[11,12] Evidence of a multiple valley structure of the valence band of $HgTe/Hg_{1-x}Cd_xTe$ quantum wells with an inverted band structure is presented. Stormer *et al.*[14] reported a distribution of holes between two spin split subbands in a *p*-type $GaAs/Al_xGa_{1-x}As$ heterojunction, due to lifting of the Kramers degeneracy at finite $\boldsymbol{k}$. In the present investigation the Kramers degeneracy is also removed; however, only one spin split subband is occupied due to the indirect band structure.

II. EXPERIMENTAL AND THEORETICAL DETAILS

The QW structures were grown by means of molecular-beam epitaxy in a Riber 2300 system which has been modified to permit the growth of Hg-based materials, as described elsewhere.[5,7,13] CdTe, Cd, Te, Hg, and Cd_3As_2 were used as source materials with typical beam equivalent pressures (b.e.p.'s) of 6×10^{-7}, 10×10^{-7}, and 2.0×10^{-4} Torr for CdTe, Te and Hg, respectively. The Cd_3As_2 b.e.p. was varied between 7×10^{-9} and 4×10^{-8} Torr. All samples were grown on (001)-oriented $Cd_{0.96}Zn_{0.04}Te$ substrates. After the growth of a 100-nm-thick CdTe buffer layer, a 40-nm-thick arsenic-doped CdTe layer was grown at the extremely low substrate temperature of 170 °C in order to enhance arsenic incorporation. This is necessary because of the low and strongly temperature dependent sticking coefficient of arsenic as reported by Yang *et al.*[15] Thereafter, a thermal activation step under a Cd flux was employed at temperatures up to 340 °C. The subsequent growth of the QW structures at substrate temperatures between 165 and 180 °C was similar to that of *n* type SQW's.[1] The QW's consist of a HgTe layer embedded between two $Hg_{0.3}Cd_{0.7}Te$ barriers. According to high-resolution x-ray-diffraction (HRXRD) measurements, layer compositions and thicknesses agree well with expected values obtained by the growth of thick epitaxial layers. All heterostructures were fully strained which was confirmed by HRXRD utilizing the asymmetric (115) Bragg reflection.

Hall bars were fabricated by means of wet chemical etching. The electrical properties of the heterostructures were

 ©2002 The American Physical Society

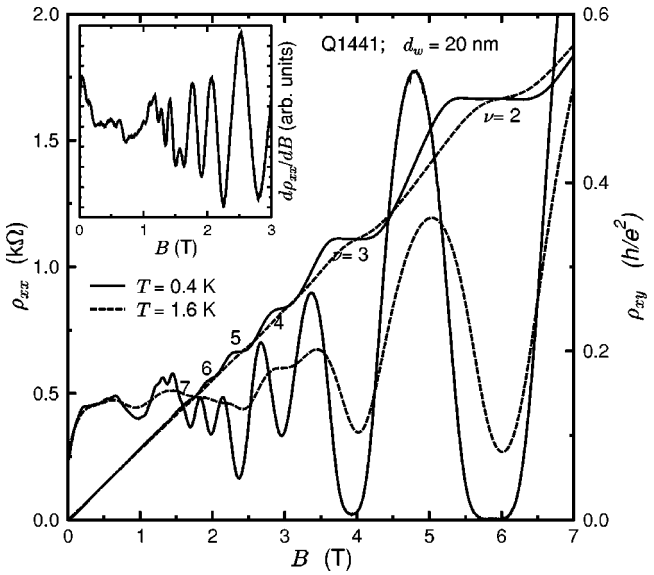

FIG. 1. The Quantum Hall effect and SdH oscillations for a *p*-type asymmetrically modulation-doped QW, Q1441, with $d_w = 20$ nm at temperatures of 0.4 and 1.6 K. $p = 2.9 \times 10^{11}$ cm^{-2} and $\mu = 1.0 \times 10^5$ cm^2/(Vs) at 0.4 K. $d\rho_{xx}/dB$ at low B is displayed in the inset.

determined via Hall-effect measurements using a standard Hall bar geometry at temperatures between 0.1 and 1.6 K and magnetic fields up to 14 T. In order to fabricate gated Hall bars, a 300-nm-thick TiO_2 layer was deposited by electron-beam evaporation, which serves as an insulating layer, before an Al layer was deposited which forms the top electrode. The QW contacts were soldered with indium whereas the top gate contact was formed with silver paste in order to avoid deterioration of the underlying heterostructure.

Transport measurements were carried out in He^4 and He^3 cryostats, as well as a He^3/He^4 dilution cryostat at temperatures between 0.1 and 1.6 K. Standard lock-in techniques using a current of $1\,\mu$A were employed. Figure 1 shows the quantum Hall effect and SdH oscillations for a *p*-type asymmetrically modulation doped QW, Q1441, with a well width d_w of 20 nm at temperatures of 0.4 and 1.6 K.

In order to understand the experimental results, self-consistent Hartree calculations were carried out. The corresponding band-structure calculations are based on Kane's $8 \times 8\boldsymbol{k}\cdot\boldsymbol{p}$ model including all second-order terms representing the remote-band contributions.[2,4] The intrinsic inversion asymmetry of HgTe and $Hg_{0.3}Cd_{0.7}Te$ is neglected, which is known to be extremely small.[16] The envelope function approximation is used to calculate the subband dispersion of the heterostructure. The influence of the induced free carriers has been included in a self-consistent Hartree calculation. For the solution of Poisson's equation it is assumed that all free carriers come from the arsenic doped CdTe layer.

For the valence band offset Λ, between CdTe and HgTe, a value of 570 meV was employed,[7] and was assumed to vary linearly with barrier composition,[17] i.e., $x\Lambda$. The relevant band structure parameters of CdTe and HgTe at $T = 0$ K are listed in Table I. The energy gap for $Hg_{0.3}Cd_{0.7}Te$ used in these calculations was taken from the empirical expression of Laurenti *et al.*[18]

TABLE I. Band-structure parameters for HgTe and CdTe employed in the calculations at $T = 0$ K in the $8 \times 8\boldsymbol{k}\cdot\boldsymbol{p}$ Kane model.

	E_g (eV)	Δ (eV)	E_p (eV)	F	γ_1	γ_2	γ_3	κ	ϵ
HgTe	−0.303	1.08	18.8	0	4.1	0.5	1.3	−0.4	21
CdTe	1.606	0.91	18.8	−0.09	1.47	−0.28	0.03	−1.31	10.4

III. RESULTS AND DISCUSSION

As alluded to above, a $HgTe/Hg_{0.3}Cd_{0.7}Te$ quantum well with a thickness d_w, less than approximately 6 nm is a semiconductor with a normal band sequence. But at larger values of d_w the QW is a semiconductor with inverted band structure as shown in Fig. 2, i.e., the $H1$ subband is now the first conduction subband, the $E1$ subband is one of the valence subbands, and the $H2$ subband is the first valence subband.[9–11] Here we shall concentrate on the inverted band structure regime.

Results of theoretical calculations[11,12] shown in Fig. 2 demonstrate that in QW's with a wide HgTe layer the first valence subband displays an electron like dispersion for small $\boldsymbol{k}_\parallel$ vectors, whereas for large $\boldsymbol{k}_\parallel$ vectors the dispersion is hole like. Consequently, instead of a valence subband maximum at the center of the Brillouin zone, maxima with fourfold symmetry are found at finite values of $\boldsymbol{k}_\parallel$. Due to the asymmetric doping of the heterostructure the charge distribution is also asymmetric which results in a lifting of the spin degeneracy for each subband for a given $\boldsymbol{k}_\parallel$ vector. As a consequence of the large heavy-hole effective mass and the

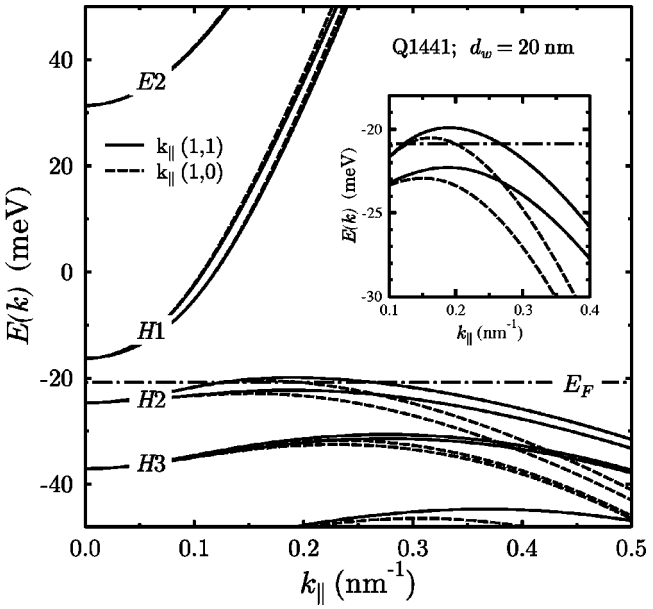

FIG. 2. The inverted band structure of a *p*-type asymmetrically modulation-doped QW, Q1441, with $d_w = 20$ nm at a temperature of 0.4 K.

resulting large density of states, only one spin component of the $H2$ subband in Q1441 is occupied by holes even for large hole densities, as shown in the inset in Fig. 2. Using the resulting potential, the Landau-level spectrum has been calculated, taking into account the full fourfold symmetry of the QW structure. This symmetry results in an anticrossing behavior for Landau levels with the same symmetry, and therefore in a very complicated spectrum for small magnetic fields.[19] At higher magnetic fields a more regular sequence of Landau levels is expected.

The hole concentration and Hall mobility for Q1441 are 2.9×10^{11} cm^{-2} and 1.0×10^{5} $cm^2/(Vs)$, respectively. Well developed quantum Hall plateaus are visible, and ρ_{xx} vanishes for the filling factor of 2 at a temperature of 0.4 K and a magnetic-field strength of about 6 T; see Fig. 1. The latter behavior is evidence of the absence of conduction due to carriers other than the two-dimensional (2D) holes in the quantum well. SdH oscillations, albeit irregular, can be seen in $d\rho_{xx}/dB$ shown in the inset at magnetic-field strengths as low as 0.2 T. In agreement with our calculations, the irregular behavior of the SdH effect at low magnetic fields turns into regular oscillations above 2 T which is characteristic of all investigated *p*-type HgTe QW's with an inverted band structure, i.e., a well width >6 nm. Noteworthy is the large increase in magnetoresistance at low magnetic field strengths, i.e., the magnetoresistance has increased by a factor of two at $B=0.2$ T. This large increase in magnetoresistance has been observed in all *p*-type HgTe QW's with an inverted band structure.

In weak-localization studies of the 2D electron gas in HgTe/CdTe superlattices and heterojunctions, Moyle *et al.*[20] observed a logarithmic anomaly in the transverse magnetoresistance near $B=0$ which arises from coherent backscattering effects with dominant spin-orbit scattering. The behavior of the transverse magnetoresistance of the 2D hole gas in the present investigation is appreciably different; ρ_{xx} at low values of B is nearly temperature independent between 0.1 and 1.6 K, see Fig. 1 [ρ_{xx}(0.1 K) is not shown], and is not a logarithmic function of magnetic field, even though its magnitude of $\Delta\rho_{xx}/\Delta B$ is considerably larger. This interesting phenomenon requires further study.

Whereas quantum effects in *n*-type samples can be observed at temperatures as high as 60 K, SdH oscillations in inverted *p*-type SQW's are strongly temperature dependent as a consequence of the large effective mass of the heavy holes. Figure 1 shows the temperature dependence of the SdH oscillations for sample Q1441 at temperatures of 0.4 and 1.6 K.

Illumination with a red light-emitting diode at low temperatures converts the *p*-type conductivity of QW Q1441 to *n* type with an electron concentration and mobility of 8×10^{10} cm^{-2} and 2.0×10^{5} $cm^2/(Vs)$, respectively. Since the *n*-type conductivity persists several hours until the sample is warmed up, we assume that persistent photoconductivity is responsible for this behavior,[21] which is beyond the scope of this investigation.

In experiments with a gated Hall bar from sample Q1645 with a QW width of 15 nm, we have been able to control the hole concentration via the gate voltage almost linearly between 3.7×10^{11} and 1.1×10^{12} cm^{-2}. Simultaneously, the Hall mobility increases with gate voltage due to screening effects to a maximum value of 6×10^{4} $cm^2/(Vs)$. Fourier analysis of the SdH oscillations results in a peak denoted p_2 in Fig. 3 which coincides with the total hole density, as determined from the Hall coefficient at low magnetic fields (filled circles) and is thus further evidence that no other charge carriers are present. A second peak p_1 is visible at small gate voltages, i.e., low hole densities.

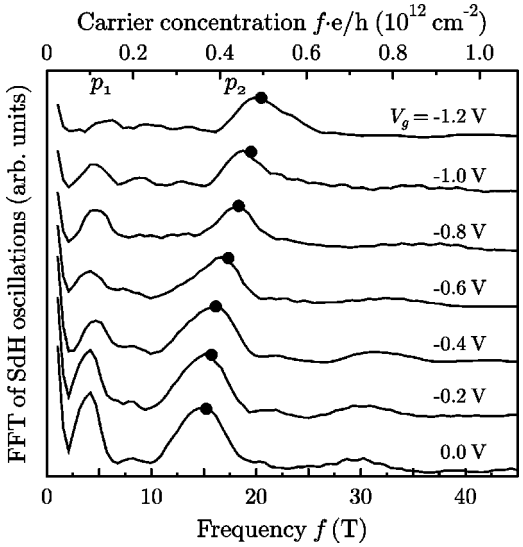

FIG. 3. FFT of SdH oscillations for the gated Hall bar from Q1645 with $d_w=15$ nm at 0.45 K. The filled circles represent the total hole density from the Hall coefficient. The peak at the frequency p_1 vanishes when the hole concentration exceeds 5×10^{11} cm^{-2}.

Within experimental uncertainties, p_2 is a factor of 4 larger than p_1. In addition, the p_1 peak vanishes when the total hole concentration exceeds 5×10^{11} cm^{-2}. This behavior can be understood by means of our theoretical model; according to our band-structure calculations,[12] the Fermi contour, which represents the occupancy of the $H2$ valence subband for an inverted QW, undergoes a transition between four equivalent areas at finite values of $\boldsymbol{k}$ shown in Fig. 4 to a region resembling a distorted ring (see Fig. 5) when the hole concentration exceeds a certain value. This transition is expected to occur at a total hole density of about 4×10^{11} cm^{-2} for a 15-nm-wide well. The disappearance of the p_1 peak can therefore be interpreted as evidence of a transition from the fourfold occupied areas or Fermi contours to that of a distorted ring. Secondary valence band maxima have been predicted by a number of investigations involving band-structure calculations;[9,10] however, previously there has been no direct experimental evidence of their existence.

In addition to this transition at relatively low hole concentrations, the behavior of SdH oscillations at higher densities is of interest. Since the maximum of the valence subband is located at finite $\boldsymbol{k}$ values, an increase in the carrier concentration is expected not only to result in an increase in the SdH oscillation frequency due to the net hole density but also in a decrease in the frequency caused by the density of

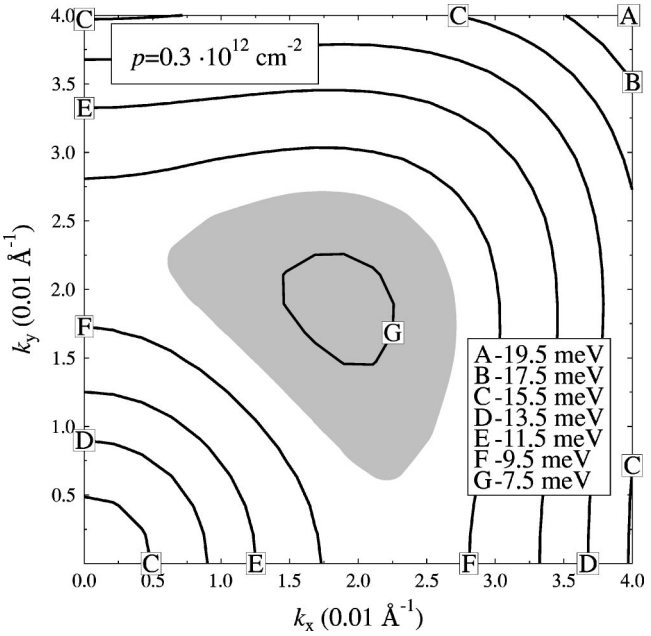

FIG. 4. Contour plot of the $H2$ valence band with the occupied states indicated by the gray area for a 15-nm-wide p-type QW, Q1645, with $p=3\times10^{11}$ cm^{-2}. The occupied region is crescent shaped and fourfold degenerate.

confined electrons. The former frequency corresponds to the negative dispersion of the outer Fermi contour, (cf. Fig. 5), whereas the latter corresponds to the positive dispersion of the inner Fermi contour. Furthermore, these two frequencies in the SdH oscillations are expected according to the predictions of density of states calculations of Landau levels in a

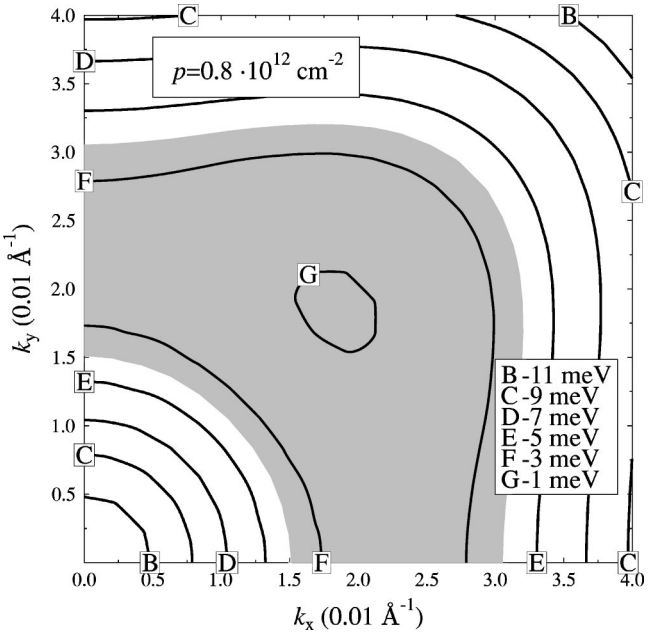

FIG. 5. Contour plot of the $H2$ valence band with the occupied states indicated by the gray area for a 15-nm-wide p-type QW, Q1645, with $p=8\times10^{11}$ cm^{-2}. Here the occupied region has the shape of a distorted ring in $\boldsymbol{k}$ space.

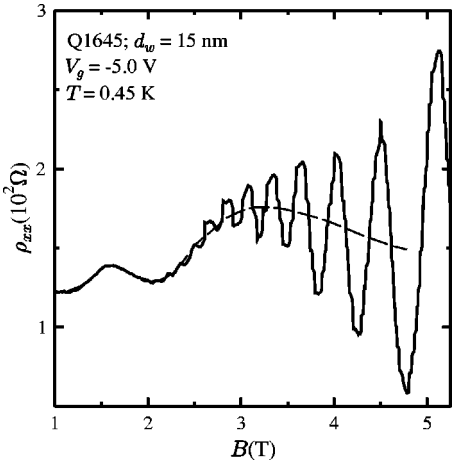

FIG. 6. SdH oscillations of a p-type QW, Q1645, with $d_w=15$ nm at a gate voltage of -5.0 V. The dashed curve which represents the mean amplitude values of the high frequency SdH oscillation reveals a low-frequency oscillation.

low order, cumulant approach (LOCA).[11,22] However the latter frequency in the SdH oscillations was clearly not observed in the corresponding fast Fourier transformation (FFT) in experiments with a gate-controlled Hall bar. This may be due to both experimental difficulties and the lack of a comprehensive transport theory. The expected oscillations of the confined electrons occur at higher carrier densities and consequently are accompanied by the higher oscillation frequency due to the hole concentration which tends to mask or obscure them. Even though the low frequency oscillation is not visible in the FFT, it can be seen in the plot of $\rho_{xx}(B)$ at a gate voltage of $V_g=-5$ V shown in Fig. 6. Here only two periods of a low frequency oscillation are visible before the oscillations are totally obscured.

For a comparison between inverted and normal semiconducting heterostructures, magnetotransport investigations have been performed on a 5.8-nm-thick p-type single QW, Q1664. In this case, band structure calculations predict a direct energy gap of about 12 meV between the $H1$ valence subband and the $E1$ conduction subband. Figure 7 shows the QHE effect and SdH oscillations measured at 1.6 K. ρ_{xx} goes to zero for filling factors of one and two, indicating the lack of conduction due to carriers other than the 2D holes in the quantum well. This behavior was observed for all investigated samples. Q1664 remains p-type up to a temperature of 150 K as a consequence of the larger energy gap compared to the 20-nm-wide QW Q1441 which is converted to n type when a temperature of 30 K is exceeded.

A Fourier analysis of the SdH oscillations (see the inset in Fig. 7) shows three distinct peaks corresponding to hole densities of 1.00, 1.95, and $2.95\pm0.05\times10^{11}$ cm^{-2}. The third peak is the sum of the first two peaks. Furthermore, this sum frequency p_{SdH} is equivalent to the total hole concentration which was determined from the Hall coefficient $p_{\mathrm{Hall}}=3.0\times10^{11}$ cm^{-2}, and is indicated by the arrow in the inset in Fig. 7. p_{SdH} and p_{Hall} have been found to be equivalent in all QW's in this study.

Self-consistent Hartree calculations depicted in Fig. 8 re-

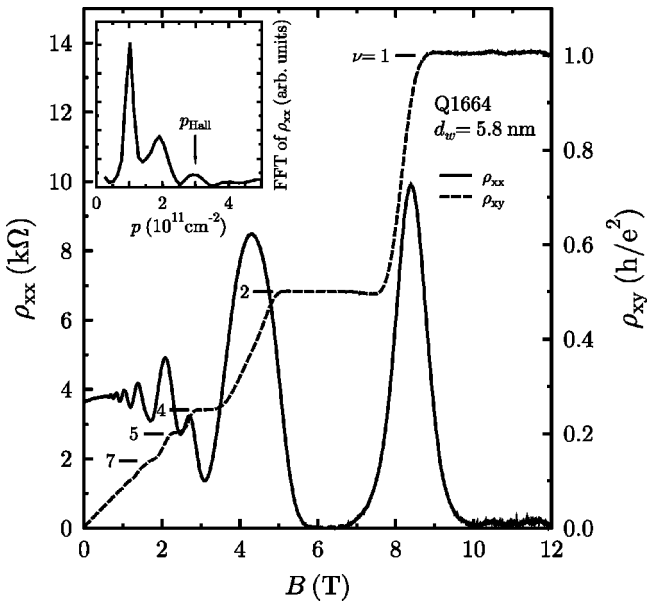

FIG. 7. Quantum Hall effect and SdH oscillations at 1.6 K for a p-type QW, Q1664, with $d_w=5.8$ nm and a direct band gap. $p=3.0\times10^{11}$ cm^{-2} and $\mu=1.5\times10^4$ cm^2/(Vs). The FFT of the SdH oscillations is shown in the inset, in which an arrow indicates the total hole density as determined from the Hall coefficient.

sult in hole concentrations of 1.01 and 0.97×10^{11} cm^{-2} for the $H1-$ and $H1+$ subbands at $\boldsymbol{k}_\parallel\approx0$, respectively. Moreover, the hole concentration of the $H1-$ subband at the secondary maxima at $\boldsymbol{k}_\parallel\approx0.5$, according to these calculations is 0.97×10^{11} cm^{-2}. For these calculations the total experimental hole concentration of 2.95×10^{11} cm^{-2} has been taken as an input parameter. It must be mentioned that the subbands are mixed at $\boldsymbol{k}_\parallel\approx0.5$, and hence this subband is no longer the pure $H1-$ subband, even though we shall continue to use this designation.

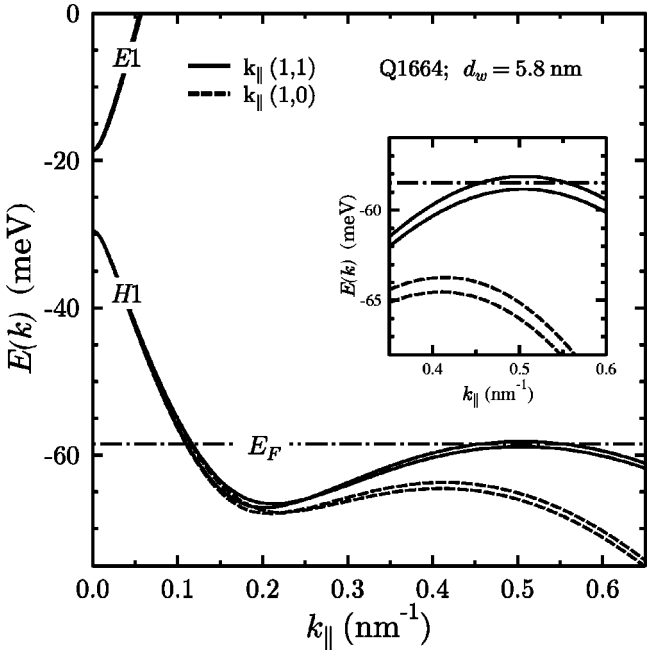

FIG. 8. Self-consistently calculated band structure of the $HgTe/Hg_{0.3}Cd_{0.7}Te$ QW, Q1664, with $d_w=5.8$ nm and $p=3.0\times10^{11}$ cm^{-2}. Although this structure has a direct energy gap, additional $H1-$ states are occupied at finite $\boldsymbol{k}$.

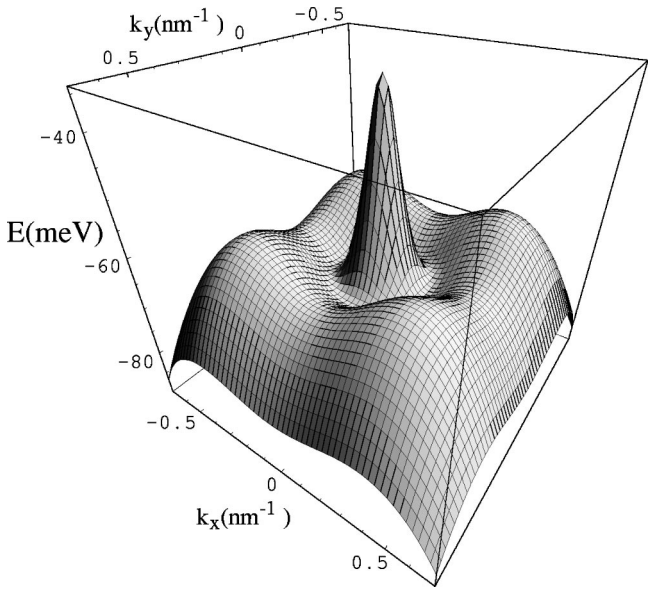

FIG. 9. 3D plot of the self-consistently calculated $H1$ subband dispersion of a QW, Q1664, with $d_w=5.8$ nm and $p=3.0\times10^{11}$ cm^{-2}. The four secondary maxima at finite $\boldsymbol{k}$ are clearly visible.

In agreement with the above calculations, the experimental peak corresponding to $p=1.00\times10^{11}$ cm^{-2} is due to the $H1-$ and $H1+$ subbands at $\boldsymbol{k}_\parallel\approx0$ as well as the $H1-$ subband at $\boldsymbol{k}_\parallel\approx0.5$. Finally the peak corresponding to $p=1.95\times10^{11}$ cm^{-2} is the sum of the hole concentrations of the spin-orbit split $H1-$ and $H1+$ subbands at $\boldsymbol{k}_\parallel\approx0$. A peak due to the four secondary maxima at $\boldsymbol{k}_\parallel(1,1)\approx0.5$ shown in Fig. 9 could be expected; however, this should occur at a very low frequency corresponding to $p=0.24\times10^{11}$ cm^{-2} and is therefore not observed.

It is noteworthy that the population difference depends on the direction in $\boldsymbol{k}$ space. In the (1,0) direction the population difference is negligible since only the subbands near $\boldsymbol{k}\approx0$ are occupied. As can also be seen in Fig. 8, the population difference is large in the (1,1) direction. Here only the $H1-$ component at $\boldsymbol{k}\approx0.5$ nm^{-1} is occupied. Since the 5.8-nm-thick QW is near the transition between normal and inverted band-structure regimes at 6 nm, the magnitude of this $\boldsymbol{k}$-space-dependent occupancy of the subbands is very sensitive to the well width in this region.

IV. CONCLUSIONS

High-mobility p-type modulation-doped HgTe single QW's have been successfully grown with arsenic as the dopant. Hole concentrations between 1.8×10^{11} and 6×10^{11} cm^{-2} and Hall mobilities up to $1.0\pm0.1\times10^5$ cm^2/(Vs) have been achieved. SdH oscillation mea-

surements at variable hole densities of a *p*-type QW with an inverted band structure show clear evidence of the existence of an indirect band gap at finite $\boldsymbol{k}$. Furthermore, experimental observations are in agreement with the predicted transition between four equivalent, unconnected Fermi surfaces and a region resembling a distorted ring. A quantitative agreement between magnetotransport and band-structure calculations has also been achieved for a narrow *p*-type SQW with a normal band structure and consequently a direct energy gap. In this case the pronounced experimental difference in occupation of the subbands is dependent on the direction in $\boldsymbol{k}$ space due to the presence of multiple secondary valleys.

ACKNOWLEDGMENTS

The support of the Deutsche Forschungsgemeinschaft via SFB 410, and the Volkswagen Foundation for one of us (X. C. Z.) is gratefully acknowledged. We also thank W. Biberacher and K. Neumaier for their experimental support in low-temperature measurements at the Walther Meissner Institut in Munich.

*Electronic address: becker@physik.uni-wuerzburg.de

[1] F. Goschenhofer, J. Gerschütz, A. Pfeuffer-Jeschke, R. Hellmig, C.R. Becker, and G. Landwehr, J. Electron. Mater. **27**, 532 (1998).

[2] A. Pfeuffer-Jeschke, F. Goschenhofer, S.J. Cheng, V. Latussek, J. Gerschütz, C.R. Becker, R.R. Gerhardts, and G. Landwehr, Physica B **256**, 486 (1998).

[3] M. von Truchsess, V. Latussek, C.R. Becker, and E. Batke, J. Cryst. Growth **159**, 1104 (1996).

[4] X.C. Zhang, A. Pfeuffer-Jeschke, K. Ortner, V. Hock, H. Buhmann, C.R. Becker, and G. Landwehr, Phys. Rev. B **63**, 245305 (2001).

[5] C.R. Becker, X.C. Zhang, K. Ortner, V. Latussek, and A. Pfeuffer-Jeschke, Proc. SPIE **4086**, 31 (2000).

[6] M. von Truchsess, V. Latussek, F. Goschenhofer, C.R. Becker, E. Batke, R. Sizmann, and P. Helgesen, Phys. Rev. B **51**, 17 618 (1995).

[7] C.R. Becker, V. Latussek, A. Pfeuffer-Jeschke, G. Landwehr, and L.W. Molenkamp, Phys. Rev. B **62**, 10 353 (2000).

[8] J.R. Meyer, C.A. Hoffman, F.J. Bartoli, J.W. Han, J.W. Cook, J.F. Schetzina, X. Chu, J.P. Faurie, and J.N. Schulmann, Phys. Rev. B **38**, 2204 (1988).

[9] C.A. Hoffman, J.R. Meyer, F.J. Bartoli, J.W. Han, J.W. Cook, J.F. Schetzina, and J.N. Schulmann, Phys. Rev. B **39**, 5208 (1989).

[10] J.R. Meyer, C.A. Hoffman, and F.J. Bartoli, Physica B **191**, 171 (1993), and references therein.

[11] K. Ortner, X.C. Zhang, S. Oehling, J. Gerschütz, A. Pfeuffer-Jeschke, V. Hock, C.R. Becker, G. Landwehr, and L.W. Molenkamp, Appl. Phys. Lett. **79**, 3980 (2001).

[12] A. Pfeuffer-Jeschke, V. Latussek, and G. Landwehr, in *Proceedings of the 9th International Conference on Narrow Gap Semiconductors*, edited by N. Puhlmann, H. U. Muller, and M. v. Ortenberg (Humboldt University at Berlin, Germany, 2000), p. 153.

[13] A. Pfeuffer-Jeschke, Ph.D. thesis, Physikalisches Institut, Universität Würzburg, Germany, 2000.

[14] H.L. Stormer, Z. Schlesinger, A. Chang, D.C. Tsui, A.C. Gossard, and W. Wiegmann, Phys. Rev. Lett. **51**, 126 (1983).

[15] B. Yang, F. Aqariden, C.H. Grein, A. Jandaska, T.S. Lee, A. Nemani, S. Rujirawat, X.H. Shi, M. Sumstine, S. Velicu, and S. Sivananthan, J. Vac. Sci. Technol. B **17**, 1205 (1999).

[16] M. H. Weiler, *Semiconductors and Semimetals*, edited by R. K. Willardson and A. C. Beer, Vol. 16 (Academic Press, New York, 1981), p. 119.

[17] C.K. Shih and W.E. Spicer, Phys. Rev. Lett. **58**, 2594 (1987).

[18] J.P. Laurenti, J. Camassel, A. Bouhemadou, B. Toulouse, R. Legros, and A. Lusson, J. Appl. Phys. **67**, 6454 (1990).

[19] G. Landwehr, J. Gerschütz, S. Oehling, A. Pfeuffer-Jeschke, V. Latussek, and C.R. Becker, Physica E (Amsterdam) **6**, 713 (2000).

[20] J.K. Moyle, J.T. Cheung, and N.P. Ong, Phys. Rev. B **35**, 5639 (1987).

[21] B. Saffian, W. Kraak, B. Oelze, H. Künzel, and J. Büttcher, Phys. Status Solidi B **196**, 323 (1996).

[22] R.R. Gerhardts, Surf. Sci. **58**, 227 (1976).